What Phasons Look Like: Particle Trajectories in a Quasicrystalline Potential

Justus A. Kromer,[1] Michael Schmiedeberg,[2,*] Johannes Roth,[3] and Holger Stark[1]

[1]*Institut für Theoretische Physik, Technische Universität Berlin, D-10623 Berlin, Germany*
[2]*Institut für Theoretische Physik 2: Weiche Materie, Heinrich-Heine-Universität Düsseldorf, D-40204 Düsseldorf, Germany*
[3]*Institut für Theoretische und Angewandte Physik, Universität Stuttgart, D-70550 Stuttgart, Germany*

Among the distinctive features of quasicrystals—structures with long-range order but without periodicity—are phasons. Phasons are hydrodynamic modes that, like phonons, do not cost free energy in the long-wavelength limit. For light-induced colloidal quasicrystals, we analyze the collective rearrangements of the colloids that occur when the phasonic displacement of the light field is changed. The colloidal model system is employed to study the link between the continuous description of phasonic modes in quasicrystals and collective phasonic flips of atoms. We introduce characteristic areas of reduced phononic and phasonic displacements and use them to predict individual colloidal trajectories. In principle, our method can be employed with all quasicrystalline systems in order to derive collective rearrangements of particles from the continuous description of phasons.

Quasicrystals are structures with long-range positional order but they do not have a unit cell which repeats in space [1,2]. Therefore, they possess rotational point symmetries that are not allowed in conventional periodic crystals. Another property that does not exist in classical crystals are the so-called phasons. They cause correlated rearrangements of atoms and are usually described in a hydrodynamic theory by a continuous mass density [3]. Like phonons, phasons are hydrodynamic modes that do not cost free energy in the long-wavelength limit. Apart from the continuous hydrodynamic description, there is a second way to delineate phasons. Especially in an atomic or tiling model, phasonic flips, i.e., the correlated jumps of atoms to new sites, are also referred to as phasons. The features of such collective flips are still a main topic of research and intensively discussed in the field [4].

The diffusive dynamics of phasonic modes influences the properties of a quasicrystal and can be detected in scattering experiments (for a recent review see, e.g., [5]). However, details of the microscopic motion of atoms due to phasonic modes are usually not resolved. There are only a few experiments which explore phasonic dynamics with atomic resolution. For example, transmission electron microscopy of an Al-Cu-Co decagonal quasicrystal revealed rearrangements of atoms due to phasonic excitations [6]. It was also observed that phasonic flips usually are strongly correlated [7]. Furthermore, strain relaxation that leads to the formation of a decagonal quasicrystal in an Al-Cu-Co-Si system is accompanied by complex collective rearrangements of atoms [8]. In general, phasonic modes contribute to thermal vibrations and thereby are important for the thermal properties of a quasicrystal. With the help of a dark-field scanning transmission electron microscopy with atomic resolution, thermal vibrations were measured in a decagonal $Al_{72}Ni_{20}Co_8$ quasicrystal revealing the importance of phasonic contributions [9]. The microscopic properties of phasonic strain relaxation were also studied in a nonlinear photonic quasicrystal [10].

However, phasonic displacements in the continuum picture and collective phasonic flips of atoms are usually employed as two independent descriptions of phasons. In this Letter, we present a method that links both pictures. Many properties of conventional periodic crystals can be deduced from a single unit cell, which does not exist in quasicrystals. Nevertheless, we are able to define characteristic areas for phononic and phasonic displacements. We demonstrate that each particle trajectory accompanying a phasonic displacement can be predicted by mapping it onto these areas.

Colloidal particles are widely used as model systems of statistical mechanics; e.g., to study crystallization, phase ordering, and dynamics in external fields [11]. Since colloids in laser fields are driven into the direction of highest light intensity [12], one can induce complex structures in a charge-stabilized colloidal suspension [13]. For example, light fields created by five interfering laser beams enforce quasicrystalline ordering of colloids [14–17]. Now, one can realize each phasonic displacement in the light interference pattern by tuning the phases of the laser beams appropriately (see also [16]). In the following, we use such phasonic displacements to explore the corresponding rearrangements or phasonic flips of our colloidal model atoms in the light-induced colloidal quasicrystal.

In case of five interfering laser beams, the light field creates an external potential with decagonal symmetry [14,18]

$$V(\mathbf{r}) = -\frac{V_0}{25} \sum_{j=0}^{4} \sum_{k=0}^{4} \cos[(\mathbf{G}_j - \mathbf{G}_k) \cdot \mathbf{r} + \phi_j - \phi_k]. \quad (1)$$

Here $\mathbf{G}_j = (2\pi \cos[2\pi j/5]/a_V, 2\pi \sin[2\pi j/5]/a_V)$ are the wave vectors projected onto the xy plane, a_V is the length scale of the potential, and ϕ_j are the phases chosen according to [3]

$$\phi_j = \mathbf{u} \cdot \mathbf{G}_j + \mathbf{w} \cdot \mathbf{G}_{3j \bmod 5}, \quad (2)$$

such that $\mathbf{u} = (u_x, u_y)$ is a phononic (i.e., a conventional) displacement and $\mathbf{w} = (w_x, w_y)$ is the phasonic displacement. We will apply a phasonic drift in order to analyze the resulting colloidal rearrangements. In the following, we denote a potential with a phasonic displacement $\mathbf{w}$ by $V_{\mathbf{w}}(\mathbf{r})$. Furthermore, we assume that the colloids are always located in local minima, which we determine by a gradient descent method. To test this assumption, we have also performed Brownian dynamics simulations. Expectedly, for large ratios of potential strength to temperature, $V_0/(k_B T)$, slow phasonic drift velocities, and only weak colloidal interactions, we observe exactly the same behavior as when we follow the minima directly.

Figure 1 and the movies in the Supplemental Material [19] show the positions of colloids when a phasonic drift is applied; i.e., when the phasonic displacement changes at a constant rate in time. The snapshots for a phasonic drift in the x direction [Fig. 1(a1)] and for a drift in the y direction [Fig. 1(b1)] illustrate the resulting complexity of the collective movement patterns of the colloids. While it is hard to recognize the correlations between the phasonic flips by employing Delaunay triangulations [see right-hand side of graphs 1(a1) and 1(b1) in Fig. 1], a better insight into the

collective dynamics is obtained by studying single trajectories. As Figs. 1(a2) and 1(b2) demonstrate, particles move in lanes. Whereas particles in the same lane proceed on average in the same direction, particles in neighboring lanes might move in the opposite direction. For a phasonic drift in the x direction, the colloidal particles either move along straight paths in the $+x$ direction or along zigzag paths in the $-x$ direction [see Fig. 1(a2)]. For a phasonic drift in the y direction, most particles follow zigzag trajectories in the $+y$ direction, but a few colloids move along stretched zigzag paths in the $-y$ direction [Fig. 1(b2)].

The last two columns of Fig. 1 show detailed snapshots of a single colloid in the decagonal potential landscape with a phasonic drift in the x direction. Depending on the starting position, the colloid either follows a straight path in the $+x$ direction [Figs. 1(c1)–1(c4)] or a zigzag path in the $-x$ direction [Figs. 1(d1)–1(d4)]. In both cases, the colloid hardly moves while it is sitting in a local minimum. When this minimum disappears at a certain phasonic displacement, the colloid slides into a new minimum. It stays there until a phasonic displacement is reached where the new minimum vanishes as well and the colloid has to slide again.

Interestingly, up to a displacement of the whole system, the potential and the position of the colloid repeat after a certain phasonic displacement. For example, the position of the colloid with respect to the potential landscape in Fig. 1(c4) corresponds to the situation in Fig. 1(c3) if the whole system is displaced in the x direction. Similarly, the
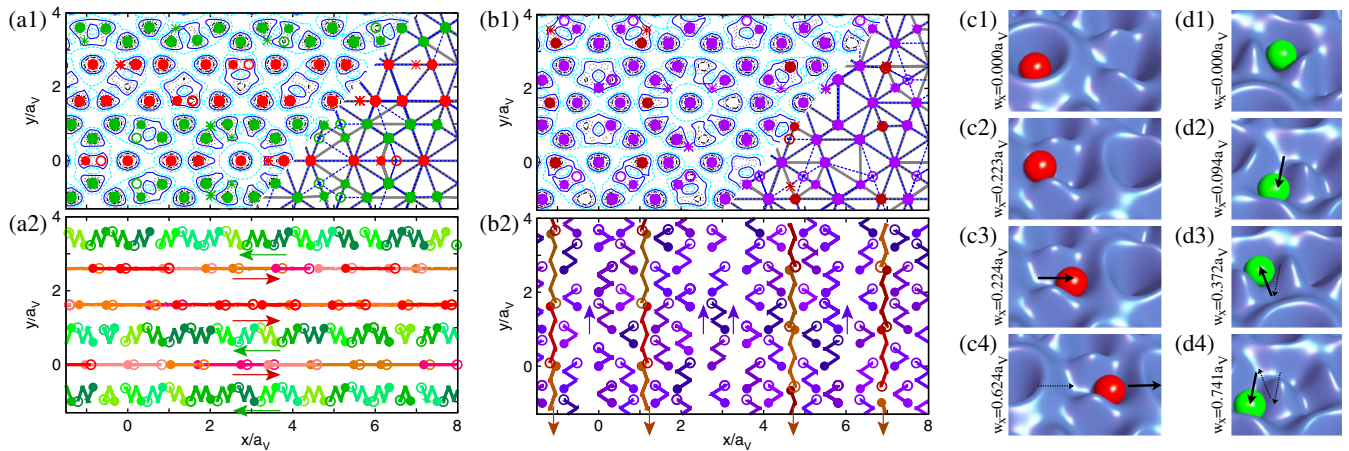

FIG. 1 (color online).   Colloidal particles located in the minima of a potential with decagonal symmetry when a phasonic drift is applied in the x direction [(a1), (a2), and (c1)–(d4)] and in the y direction [(b1) and (b2)] (cf. movies in the Supplemental Material [19]). Colloids are plotted in a similar color when they move, on average, in the same direction. (a1) Snapshots for $\mathbf{w} = (0.05, 0)$ and (b1) $\mathbf{w} = (0, 0.05)$ (solid circles). The previous positions of the colloids at $\mathbf{w} = (0, 0)$ are marked by stars, the future positions by open circles at (a1) $\mathbf{w} = (0.1, 0)$ and (b1) $\mathbf{w} = (0, 0.1)$. The right parts show the Delaunay triangulation for the current and future colloidal positions by gray solid and blue dashed lines, respectively. Trajectories of the colloids for a phasonic drift from $\mathbf{w} = (0, 0)$ (solid circles) to (a2) $\mathbf{w} = (1, 0)$ or to (b2) $\mathbf{w} = (0, 1)$. (c1)–(d4) Single colloids in the decagonal landscape when a phasonic drift in the x direction is applied. Due to different starting positions, the trajectories in (c1)–(c4) are straight and point in the $+x$ direction, while the ones in (d1)–(d4) have the zigzag shape and point in the $-x$ direction. First, the colloids are in a local minimum and hardly move [see, e.g., (c1) and (c2) for the straight path]. However, with increasing phasonic displacement the minimum disappears and the colloids slide into a newly appearing minimum [see (c2), (c3), (d1), and (d2)].

zigzag path repeats with a displacement in the $-x$ direction after the colloid has slid twice [cf. Figs. 1(d2) and 1(d4)]. As a consequence, in order to understand these trajectories, it is sufficient to study one or two slides of the colloid and how these slides repeat. In general, as we will show in the next paragraphs, the trajectory of each colloid can be deduced from the motion of a colloid close to the origin in a potential with a small phasonic displacement. In the following, we will first derive how each colloid can be mapped onto such a particle close to the origin and then study its behavior when a phasonic drift is applied.

There are combinations of phononic and phasonic displacements that do not change the potential in Eq. (1). For example, for all integer numbers n, m, and $j = 0, 1, .., 9$ displacements with

$$\Delta \mathbf{u} = (u_r \cos[j\pi/5], u_r \sin[j\pi/5]),$$

$$\text{where } u_r = \frac{2}{5}a_V n + \left(\frac{1}{5} + \frac{1}{\sqrt{5}}\right)a_V m, \quad \text{and}$$

$$\Delta \mathbf{w} = (w_r \cos[3j\pi/5], w_r \sin[3j\pi/5]),$$

$$\text{where } w_r = \frac{2}{5}a_V n + \left(\frac{1}{5} - \frac{1}{\sqrt{5}}\right)a_V m \quad (3)$$

change all possible differences of phases $\phi_j - \phi_k$ only by integer multiples of 2π and therefore the potential is not modified; i.e., $V_{\mathbf{w}+\Delta\mathbf{w}}(\mathbf{r} + \Delta\mathbf{u}) = V_{\mathbf{w}}(\mathbf{r})$. Note while the phononic and phasonic displacements in Eq. (3) always occur along the symmetry axes of the potential, they do not share the same direction, in general. A phononic displacement in the direction $\alpha = j\pi/5$ is accompanied by a phasonic displacement in direction $\alpha_w = 3\alpha = 3j\pi/5$. The displacement vectors of Eq. (3) can also be employed for any mass density distribution or field with pentagonal or decagonal symmetry if this field only depends on the phase differences $\phi_j - \phi_k$ as in Eq. (2).

The properties of a colloid in a potential do not change when the position is displaced by $\Delta\mathbf{u}$ and at the same time the phasonic displacement is altered by $\Delta\mathbf{w}$ if $\Delta\mathbf{u}$ and $\Delta\mathbf{w}$ obey Eq. (3). Therefore, we can map all colloids onto particles inside a characteristic area close to the origin in a potential with only a small phasonic displacement. In the following, a colloid at a position $\mathbf{r}$ in a laser field $V_{\mathbf{w}}(\mathbf{r})$ is mapped onto a particle at a reduced position $\mathbf{r}^{(\mathrm{red})} = \mathbf{r} - \Delta\mathbf{u}$ in a potential $V_{\mathbf{w}^{(\mathrm{red})}}(\mathbf{r}^{(\mathrm{red})})$ with a reduced phasonic displacement $\mathbf{w}^{(\mathrm{red})} = \mathbf{w} + \Delta\mathbf{w}$ where $\Delta\mathbf{u}$ and $\Delta\mathbf{w}$ are chosen such that $\mathbf{r}^{(\mathrm{red})}$ and $\mathbf{w}^{(\mathrm{red})}$ are close to the origin. Since the displacements in Eq. (3) always act along the symmetry axes, the reduced position and the reduced phasonic displacement can be chosen such that $|\mathbf{r}^{(\mathrm{red})} \cdot \mathbf{e}_j| \leq (1 + \sqrt{5})a_V/10$ and $|\mathbf{w}^{(\mathrm{red})} \cdot \mathbf{e}_j| \leq (1 + \sqrt{5})a_V/10$ for any unit vector $\mathbf{e}_j = (\cos[j\pi/5], \sin[j\pi/5])$ with $j = 0, 1, .., 9$. Therefore, $\mathbf{r}^{(\mathrm{red})}$ and $\mathbf{w}^{(\mathrm{red})}$ end up in areas that are surrounded by black decagons labeled with an a in Fig. 2. To
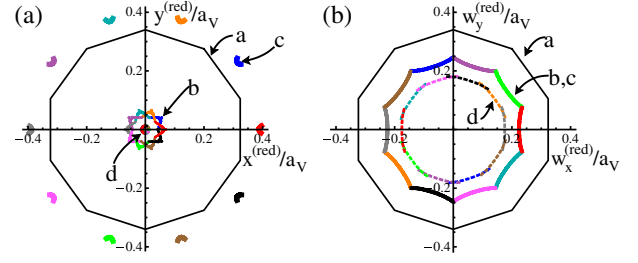

FIG. 2 (color online).   Area of (a) reduced positions $\mathbf{r}^{(\mathrm{red})}$ and (b) reduced phasonic displacements $\mathbf{w}^{(\mathrm{red})}$. The borders of the characteristic area to which all colloids can be mapped are the black decagons marked with an a. The reduced displacements of all potential minima, $\mathbf{r}^{(\mathrm{red})}$ and $\mathbf{w}^{(\mathrm{red})}$, lie in the region which is bordered by the solid colored lines labeled b. A minimum disappears when it reaches the lines b from inside the region. A colloid sitting in such a minimum slides from the lines b to the colored segments c outside the decagon. It is then mapped back into the characteristic decagonal area in a region bordered by lines marked with d. With the help of both diagrams, the trajectory of a particle in response to a phason displacement in the quasicrystalline potential can be predicted as described in the text and demonstrated in Fig. 3 for specific examples. All colored lines in the figure are determined by numerically analyzing the potential for all possible directions of the reduced phasonic displacement.

understand the behavior of a colloid in a potential with phononic and phasonic displacements, only the colloids with reduced positions $\mathbf{r}^{(\mathrm{red})}$ in potentials with $\mathbf{w}^{(\mathrm{red})}$ have to be studied. By numerically investigating all of these reduced positions and phasonic displacements, we find the following: all local minima as possible locations of colloids have reduced displacements $\mathbf{r}^{(\mathrm{red})}$ and $\mathbf{w}^{(\mathrm{red})}$ that are within the areas surrounded by the colored lines labeled b in Fig. 2. The results presented in the next paragraphs are obtained by analyzing the potential for $\mathbf{w}^{(\mathrm{red})}$ at positions $\mathbf{r}^{(\mathrm{red})}$ within this region because every colloid in a local minimum can be mapped into it.

The reduced phasonic displacement $\mathbf{w}^{(\mathrm{red})}$ changes at the same rate as the phasonic displacement $\mathbf{w}$ while inside its characteristic area and inside the region where local minima exist. However, ultimately $\mathbf{w}^{(\mathrm{red})}$ reaches one of the colored solid lines labeled b in Fig. 2(b). These lines were determined numerically and denote the reduced phasonic displacements where the potential minimum, in which the colloid sits, disappears, and therefore, the colloid slides into another local minimum. We find that the direction of sliding depends on the direction of the phasonic displacement. If $\alpha_w^{(\mathrm{red})}$ is the direction along the symmetry axes that is closest to $\mathbf{w}^{(\mathrm{red})}$, the old, as well as the new, position of the colloid are located close to the direction $\alpha^{(\mathrm{red})}$ such that $\alpha_w^{(\mathrm{red})} = 3\alpha^{(\mathrm{red})}$. In Fig. 2(a), the possible old reduced positions are shown by lines labeled b, and the new positions are outside of the characteristic decagonal at the spots marked by c. The direction of the jump can be identified by

the color, which we choose to be the same in Figs. 2(a) and 2(b). For example, when $\mathbf{w}^{(red)}$ reaches the green line marked by b in Fig. 2(b), the old and the new position are shown with the same color in Fig. 2(a). Since the new colloid position is outside of the characteristic area, we employ $\Delta\mathbf{u} = -\frac{2}{5}(\cos[\alpha^{(red)}], \sin[\alpha^{(red)}])/a_V$ and $\Delta\mathbf{w} = -\frac{2}{5}(\cos[\alpha_w^{(red)}], \sin[\alpha_w^{(red)}])/a_V$, which is a combination allowed according to Eq. (3). The new $\mathbf{r}^{(red)}$ and $\mathbf{w}^{(red)}$ are located on the colored lines marked by d in Fig. 2. Further increasing the phasonic displacement $\mathbf{w}$ repeats the whole process described in this paragraph by starting from the new reduced quantities. Therefore, Fig. 2 allows us to predict the complete path of a colloid in a potential with phasonic drift for all possible starting positions and all possible directions of the phasonic drift.

Figure 3 demonstrates how we employ our method to predict colloidal trajectories for phasonic drifts in the x or y directions. The colloid is characterized by its reduced position $\mathbf{r}^{(red)}$ and its reduced phasonic displacement $\mathbf{w}^{(red)}$. Usually, the real and the reduced particle position change in the same way. Only when $\mathbf{r}^{(red)}$ and $\mathbf{w}^{(red)}$ are mapped back onto values closer to the origin, the real position $\mathbf{r}$ is not affected at all. We obtain a colloidal trajectory by repeating the steps introduced in the previous paragraph. A detailed description is given in the caption of Fig. 3. Note that the type of the trajectory depends on the starting value of $\mathbf{w}^{(red)}$. The crosshatched areas in Figs. 3(a3), 3(b3), 3(c3), and 3(d3) denote all starting values that lead to the type of trajectory depicted in the corresponding column of the figure.

Particle trajectories in various quasicrystalline systems can be predicted by using diagrams like the one in Fig. 2. For all pentagonal or decagonal quasicrystals, characteristic areas with decagonal shape exist. In quasicrystals with other rotational symmetries, they assume suitable polygonal shapes. To obtain the details within the characteristic
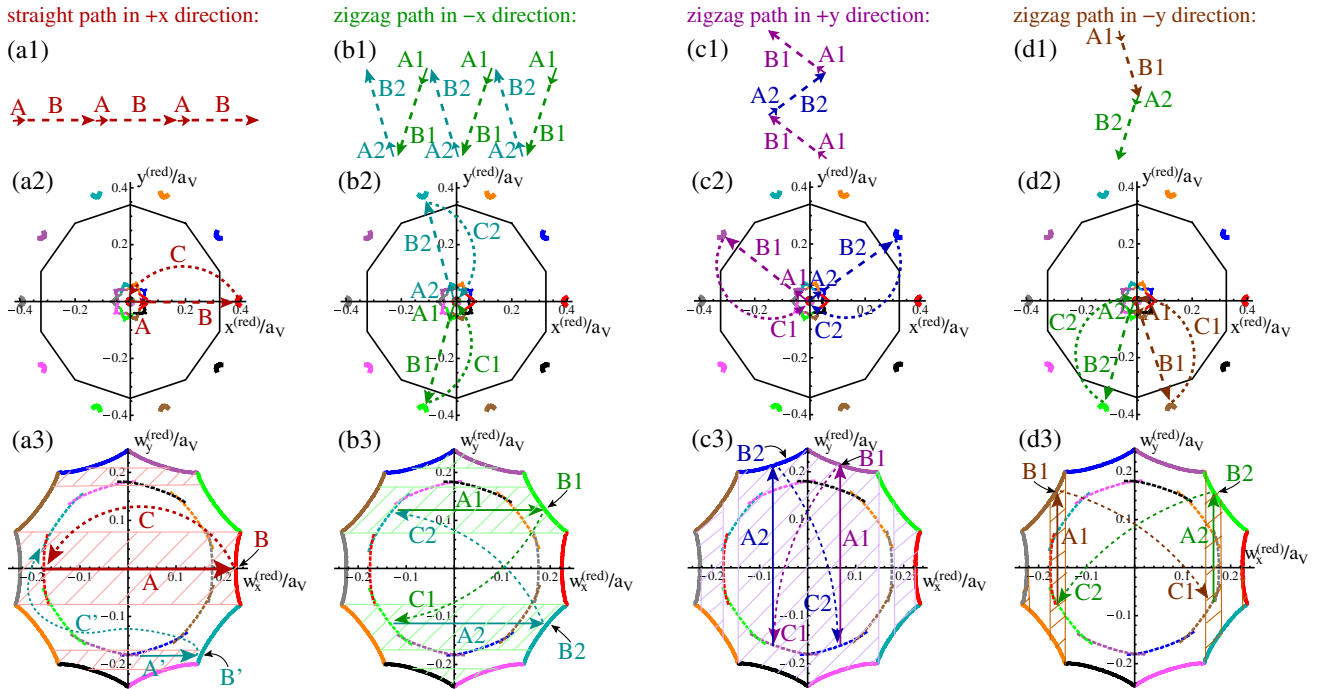

FIG. 3 (color online). Selected trajectories and how they can be predicted by employing the diagrams of Fig. 2 for particles in a potential with a phasonic drift in the x direction [(a1)–(b3)] and in the y direction [(c1)–(d3)]. Each column describes a trajectory for a starting condition where in the beginning $\mathbf{w}^{(red)}$ is within the crosshatched area. The first line [(a1), (b1), (c1), and (d1)] shows the path of the colloid, the second line [(a2), (b2), (c2), and (d2)], the corresponding reduced positions $\mathbf{r}^{(red)}$, and the last line [(a3), (b3), (c3), and (d3)], the reduced phasonic displacements $\mathbf{w}^{(red)}$. First, $\mathbf{r}^{(red)}$ changes only slightly while the phasonic displacement (either w_x or w_y) is increased (see arrows labeled A, A', $A1$, or $A2$). The local minimum that is occupied by the colloid disappears when $\mathbf{w}^{(rred)}$ reaches the colored solid border. As a consequence, the colloid slides into another local minimum depicted by the same color (see labels B, B', $B1$, or $B2$). Since the new $\mathbf{r}^{(red)}$ is outside the characteristic decagonal area, in the next step (see C, C', $C1$, or $C2$) $\mathbf{r}^{(red)}$ and $\mathbf{w}^{(red)}$ are mapped back such that $\mathbf{r}^{(red)}$ is close to the origin. Note that the real position $\mathbf{r}$ does not change due to this mapping. Afterwards, all steps are repeated for the new reduced quantities. In the case of the zigzag paths, $\mathbf{r}^{(red)}$ and $\mathbf{w}^{(red)}$ end up at their starting values after two slides (six steps: $A1$, $B1$, $C1$, $A2$, $B2$, $C2$) and in case of the straight path [(a1)–(a3)], after one slide (steps A, B, C). For some starting positions the very first steps might differ from the following ones; e.g., the steps A', B', and C' shown in (a3) do not repeat but are followed by the usual steps of a straight path. We present paths (b1)–(b3) and (c1)–(c3) in movies in the Supplemental Material [19].

area, the extrema of the field or density distribution inside the characteristic area have to be analyzed.

In this Letter, we have studied particle trajectories in a quasicrystalline potential with a global phasonic drift. In the future, we want to apply our method to determine particle motion that is caused by phasonic modes with nonzero wavelengths. For example, adatoms on the surface of a quasicrystal experience a two-dimensional quasicrystalline potential (see, e.g., [20]) where phasonic modes are thermally activated. Our method also applies to intrinsic quasicrystals; e.g., in atomic systems. Such systems are characterized by continuous density distributions, which have to be analyzed instead of an external potential. Real atoms are located at the most pronounced maxima of the density distributions. Therefore, if one analyzes the positions of these maxima within the characteristic area of reduced position and phasonic displacement, one can predict phason-induced rearrangements of atoms. One thereby links collective patterns of phasonic flips to phasonic displacements of a continuous density distribution.

*Corresponding author.
schmiedeberg@thphy.uni-duesseldorf.de

[1] D. Shechtman, I. Blech, D. Gratias, and J. W. Cahn, Phys. Rev. Lett. **53**, 1951 (1984).

[2] D. Levine and P. J. Steinhardt, Phys. Rev. Lett. **53**, 2477 (1984).

[3] D. Levine, T. C. Lubensky, S. Ostlund, S. Ramaswamy, P. J. Steinhardt, and J. Toner, Phys. Rev. Lett. **54**, 1520 (1985).

[4] C. L. Henley, M. de Boissieu, and W. Steurer, Philos. Mag. **86**, 1131 (2006).

[5] M. de Boissieu, Isr. J. Chem. **51**, 1292 (2011).

[6] K. Edagawa, K. Suzuki, and S. Takeuchi, Phys. Rev. Lett. **85**, 1674 (2000).

[7] K. Edagawa, K. Suzuki, and S. Takeuchi, J. Alloys Compd. **342**, 271 (2002).

[8] K. Edagawa, P. Mandal, K. Hosono, K. Suzuki, and S. Takeuchi, Phys. Rev. B **70**, 184202 (2004).

[9] E. Abe, S. J. Pennycook, and A. P. Tsai, Nature (London) **421**, 347 (2003).

[10] B. Freedman, G. Bartal, M. Segev, R. Lifshitz, D. N. Christodoulides, and J. W. Fleischer, Nature (London) **440**, 1166 (2006); B. Freedman, R. Lifshitz, J. W. Fleischer, and M. Segev, Nature Mater. **6**, 776 (2007).

[11] H. Löwen, J. Phys. Condens. Matter Lett. **13**, R415 (2001).

[12] A. Ashkin, Phys. Rev. Lett. **24**, 156 (1970); A. Ashkin, Science **210**, 1081 (1980).

[13] M. M. Burns, J. M. Fournier, and J. A. Golovchenko, Science **249**, 749 (1990).

[14] M. Schmiedeberg, J. Roth, and H. Stark, Eur. Phys. J. E **24**, 367 (2007).

[15] J. Mikhael, J. Roth, L. Helden, and C. Bechinger, Nature (London) **454**, 501 (2008); J. Mikhael, M. Schmiedeberg, S. Rausch, J. Roth, H. Stark, and C. Bechinger, Proc. Natl. Acad. Sci. U.S.A. **107**, 7214 (2010); J. Mikhael, G. Gera, T. Bohlein, and C. Bechinger, Soft Matter **7**, 1352 (2011).

[16] M. Schmiedeberg and H. Stark, Phys. Rev. Lett. **101**, 218302 (2008); M. Schmiedeberg, J. Mikhael, S. Rausch, J. Roth, L. Helden, C. Bechinger, and H. Stark, Eur. Phys. J. E **32**, 25 (2010).

[17] C. Reichhardt and C. J. Olson Reichhardt, Phys. Rev. Lett. **106**, 060603 (2011).

[18] S. P. Gorkhali, J. Qi, and G. P. Crawford, J. Opt. Soc. Am. B **23**, 149 (2006).

[19] See Supplemental Material at http://link.aps.org/supplemental/10.1103/PhysRevLett.108.218301 for movies.

[20] R. McGrath, J. Ledieu, E. J. Cox, and R. D. Diehl, J. Phys. Condens. Matter Lett. **14**, R119 (2002).